Parasites and climate synchronize red grouse populations

Isabella M. Cattadori[1], Daniel T. Haydon[2] & Peter J. Hudson[1]

[1]*Center for Infectious Diseases Dynamics, Mueller Laboratory, The Pennsylvania State University, University Park, Pennsylvania 16802, USA*
[2]*Division of Environmental and Evolutionary Biology, University of Glasgow, Glasgow G12 8QQ, UK*

There is circumstantial evidence that correlated climatic conditions can drive animal populations into synchronous fluctuations in abundance[1–5]. However, it is unclear whether climate directly affects the survival and fecundity of individuals, or indirectly, by influencing food and natural enemies. Here we propose that climate affects trophic interactions and could be an important mechanism for synchronizing spatially distributed populations. We show that in specific years the size of red grouse populations in northern England either increases or decreases in synchrony. In these years, widespread and correlated climatic conditions during May and July affect populations regionally and influence the density-dependent transmission of the gastrointestinal nematode *Trichostrongylus tenuis*, a parasite that reduces grouse fecundity[6]. This in turn forces grouse populations into synchrony. We conclude that specific climatic events may lead to outbreaks of infectious diseases or pests that may cause dramatic, synchronized changes in the abundance of their hosts.

Nonlinear interactions between climate and population size can influence not only temporal changes in abundance but can also lead to spatial synchrony at a range of scales[1–5,7,8]. About 50 years ago, Moran[9] proposed that uncoupled populations with identical linear density-dependent structure will asymptotically synchronize in phase under the influence of correlated environmental perturbations, and the correlation between populations will equal the correlation between the extrinsic factors. Since Moran suggested his theorem, researchers have looked for evidence of the 'Moran effect' across animal taxa and investigated how environmental noise interacts with nonlinear population dynamics, the 'nonlinear Moran effect'[2,8,10]. However, researchers have yet to identify the underlying process that generates correlated fluctuations between populations in any natural system. In populations in which fluctuations are driven by a trophic interaction, such as predator—prey, host–parasitoid or host–parasite interactions, the correlated climatic effects may operate either on these density-dependent mechanisms or more directly on population abundance, and thus move populations into a synchronous phase. Here we examine this hypothesis in the natural system of the red grouse (*Lagopus lagopus scoticus*) and its gastrointestinal parasite *Trichostrongylus tenuis*, a nematode known to play a major role in reducing fecundity and destabilizing grouse populations[6,11,12].

We used 91 time series of annual red grouse harvesting data obtained from managed grouse moors in northern England between 1839 and 1994 and collected by The Game Conservancy Trust (Fig. 1). Red grouse harvest data have proved to be a fair reflection of spatio-temporal changes in population density and annual productivity[13]. The majority (59%) of these time series exhibit cyclic fluctuations with an average period of 7 years (range 3–13 years)[14,15]. Each grouse population is embedded within one of five discrete regions of contiguous habitat[15] and we analysed synchrony between populations in each of these regions. Common statistical techniques can be used to identify spatial synchrony[16] and provide an estimate of average synchrony between time series, but they fail to identify the years in which time series are forced into synchrony. To achieve this, the dynamical state of each red grouse population was represented in a state-based Markov chain model that described temporal transitions between four phase states based on three consecutive years of observations: a cycle trough, a consecutive increase, a cycle peak and a consecutive decrease. For each region, we examined changes in the annual proportion of populations in each state, which allowed us to identify the years in which populations were forced into significant state-synchrony and quantify the state that these populations converge onto, in these years[17]. As an annual index of state synchrony among populations within each of the five regions, we applied the Shannon–Weaver diversity index to the proportion of populations in each state[17]. Populations were considered to be in synchrony when the diversity index deviated below the lower 95% confidence interval predicted by the Markov state transition model under the null hypothesis of no coupling between populations. Hence, a synchronous year can arise either as a dynamically predictable episode, as a consequence of synchrony in the preceding year, or as an unpredicted 'collective forcing episode' (CFE) that brings previously asynchronous populations into the same synchronous state[8,10]. To identify years when these forcing events occurred, we calculated whether the diversity index fell outside the one-step 95% confidence interval, conditional on the state configuration in the previous year[17]. We focused our analyses on the years in which these forcing events occurred and looked for the putative synchronizing mechanism.

The diversity index calculated among populations within each of the five regions revealed that no regular pattern characterized the incidence of the forcing episodes (Fig. 2a). The majority of populations converged on a common dynamical state: 'upward' CFEs—either two successive years of increased abundance (32% of CFEs) or peaks (32% of CFEs)—or, less frequently, 'downward' CFEs—when populations converged on two successive years of population decline (8% of CFEs) or a trough (28% of CFEs) (Fig. 2b). On the basis of knowledge of the red grouse system, we propose that there are two major demographic circumstances that would tend to generate such collective forcing episodes in these harvesting data:

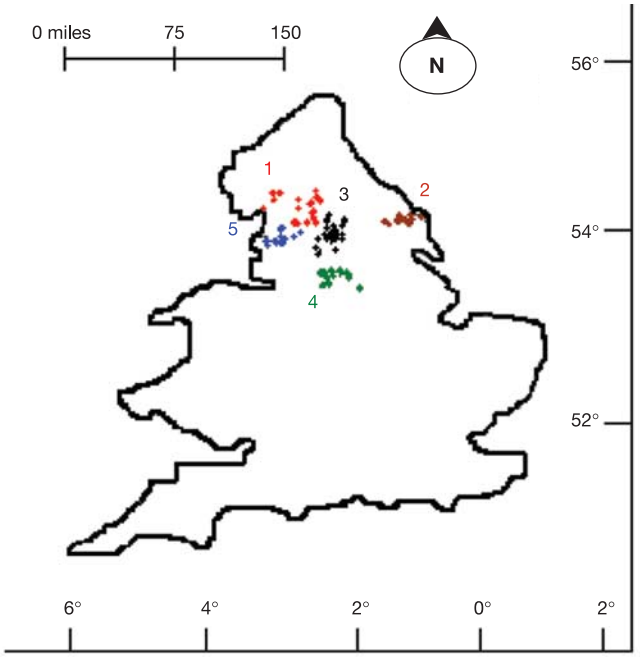

Figure 1 Locations of the 91 red grouse populations that provided annual harvesting records between 1839 and 1994. Populations were aggregated into five geographically distinct regions of contiguous grouse habitat (heather-dominant moorland), each represented here by a different colour. Synchrony between populations was examined within each of these distinct regions.

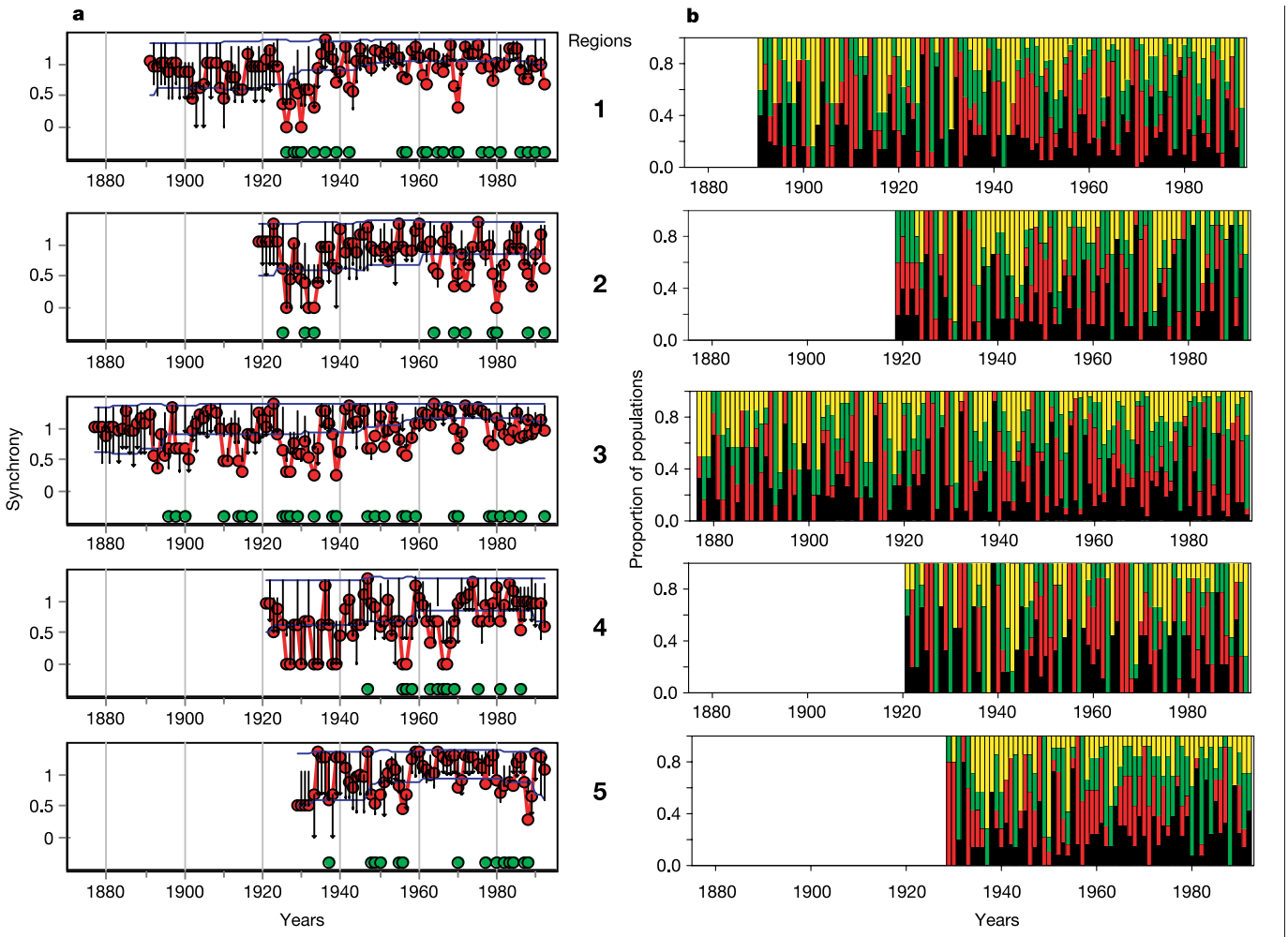

Figure 2 Spatio-temporal patterns of synchrony between populations within each of the five regions. **a**, The observed average state synchrony among populations (red line) expressed as the Shannon–Weaver index with the 95% confidence envelope (blue lines). Years in which CFEs forced the populations into an unexpected synchronous state are shown with green circles. These years were identified by predicting the expected average state of the populations conditional on the average state configurations observed the previous year and estimating their 95 percentile interval (black bars)[17]. **b**, The proportion of populations observed in each state phase in each year. Troughs are shown in black, increases in red, peaks in green and decreases in yellow. Note that in collective forcing years the populations tend to enter the same state phase. For each region, phase synchrony and the proportion of phase states were calculated using sample sizes of at least five time series per year.

first, good breeding years in which populations undergo positive growth rates (increases or peaks) and second, poor breeding years when populations experience negative growth rates (decreases or troughs). Replicated field experiments have shown that the intensity of the nematode *T. tenuis* infection has a consistent and negative impact on female fecundity, clutch size, hatching success and chick survival[11,18]. This parasite inhabits the blind-ending caeca of the grouse and has a direct life cycle. Eggs pass out of the host in the caecal faeces and in wet and warm conditions develop into a third-stage infective larva that ascends the heather and is ingested by a feeding grouse[19]. Temperature increases the development rate of the free-living stages and sufficient humidity is necessary for infection to be effective[19–21]. Climatic conditions can also directly influence the survival of grouse chicks. Dry, warm weather in May, when chicks hatch, allows them to forage and grow, whereas chicks that hatch during cold, rainy periods have less foraging time and increased mortality[22]. Intrinsic processes such as changes in spacing behaviour late in the year may also influence grouse populations[23]. However, experimental evidence has shown that such processes act at a local scale and are not associated with food and weather[24], and consequently are unlikely to be involved in generating the large-scale intermittent collective forcing episodes and the pattern of synchrony that we have observed.

To identify the environmental variables that could force populations into synchrony, we applied a generalized logistic regression model which predicted the occurrence of annual forcing episodes as a function of the intensity of parasite infection and the climatic

Table 1 **Environmental variables affecting CFEs in red grouse dynamics**

	Coefficients ± standard error	Wald test	*P*
Total May rainfall (mm)	−0.11 ± 0.02	23.76	0.001
Total July rainfall (mm)	0.15 ± 0.04	12.85	0.001
Mean May temperature (°C)	−0.83 ± 0.20	17.27	0.001
Mean July temperature (°C)	0.88 ± 0.23	14.57	0.001
Mean parasite intensity (worm/host)	0.53 ± 0.20	7.17	0.001
Variables not in the model			
Total June rainfall (mm)	0.02 ± 0.02	1.49	0.22
Total August rainfall (mm)	−0.01 ± 0.01	0.08	0.78
Mean June temperature (°C)	−0.06 ± 0.24	0.07	0.79
Mean August temperature (°C)	−0.32 ± 0.19	2.93	0.09

Generalized logistic multiple regression model: backward stepwise. Degrees of freedom = 350; log-likelihood = −125.22.

Table 2 **Mean of environmental variables in synchronous 'upwards' and 'downwards' collective forcing years**

	Upwards ± standard error ($n = 35$)	Downwards ± standard error ($n = 23$)	Mann–Whitney P
Total May rainfall (mm)	36.39 ± 1.21	47.75 ± 1.10	0.001
Total July rainfall (mm)	23.12 ± 0.81	19.47 ± 0.88	0.01
Mean May temperature (°C)	10.72 ± 0.15	10.05 ± 0.15	0.01
Mean July temperature (°C)	14.46 ± 0.16	15.95 ± 0.36	0.01
Parasite intensity (worm/host)	7.01 ± 0.14	7.50 ± 0.13	0.01

In 'upwards' collective forcing years, red grouse synchronize in peak or increase states; in 'downwards' collective forcing years, red grouse synchronize in decrease or trough states.

variables that have a major impact on breeding[11,15,25]. This model indicated that parasite intensity and the rainfall and temperature during July promoted CFEs, while May rainfall and temperature repressed CFEs (Table 1). We examined two alternative hypotheses: first, that the direct effects of correlated climatic conditions on the grouse generate CFEs (the climate hypothesis), and second, that climate indirectly influences grouse dynamics through its effect on parasite transmission (the climate–parasite hypothesis).

A structural equation framework[26,27], based on the environmental variables selected by the logistic regression, was used to compare these hypotheses. For the climate hypothesis the model consisted of rainfall and mean temperature in May and July with direct effects on grouse abundance, whereas for the climate–parasite hypothesis these climatic variables influenced the grouse both directly and indirectly through the net rate of parasite transmission, as measured by changes in parasite intensity in the host. These environmental variables differed consistently between the 'upward' and 'downward' synchronous forcing events such that Mays were dryer, Julys were wetter and parasite intensity was lower during the grouse 'upward' CFEs, whereas the pattern was reversed in the 'downward' CFEs (Table 2). Consequently, both models were fitted to these data. The two parsimonious models—based on the climate (Fig. 3a and b)

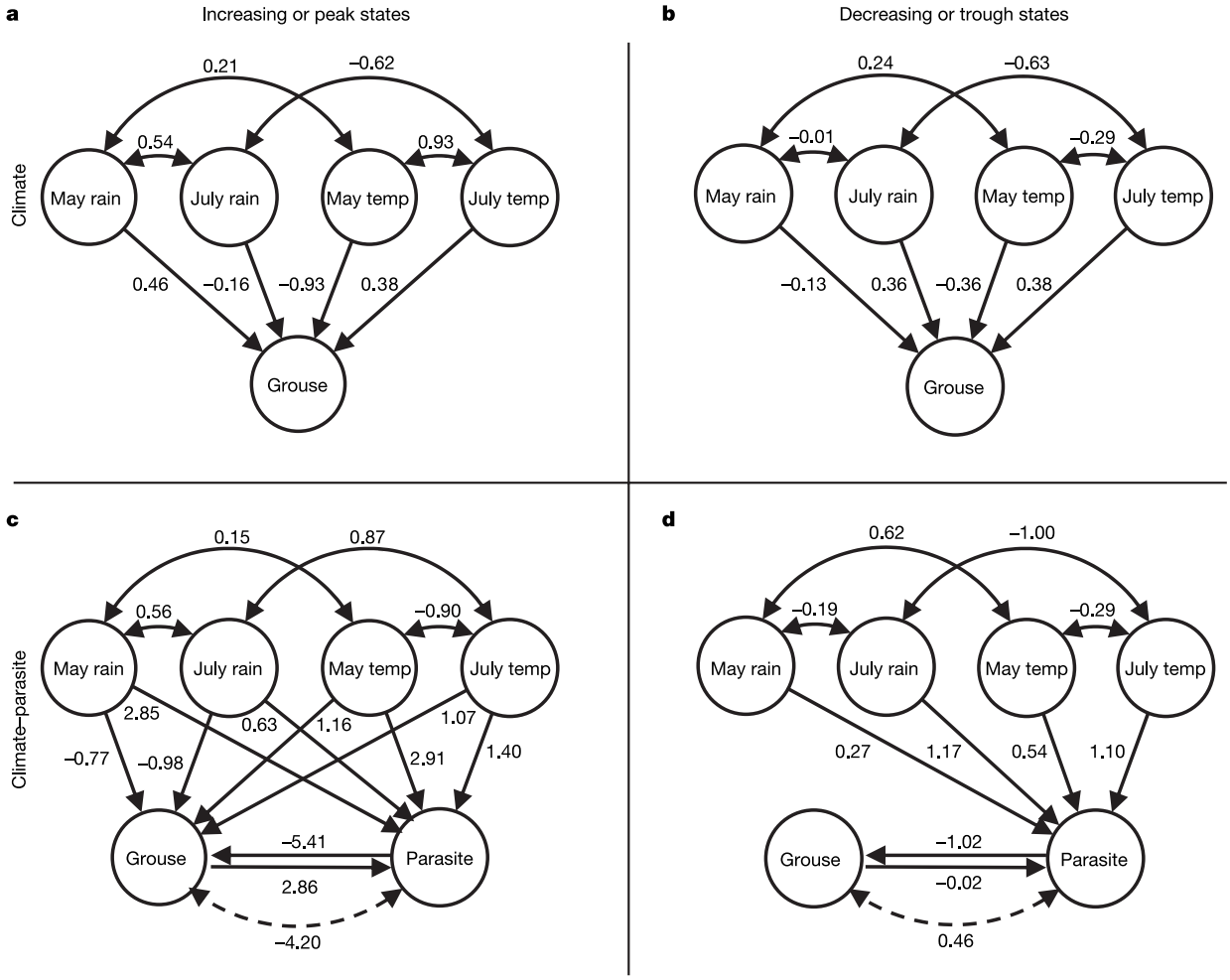

Figure 3 Simplified path diagram with parameterized path coefficients of simulated interactions between climate, parasites and red grouse. Explanatory variables describing each latent variable, the residual variance of each variable and the environmental noise of grouse and parasite variables are not represented[26]. Circles, estimated latent variables. Curved double arrows, correlated variables; dotted and curved double arrows, variables affected by correlated environmental noise; single arrows, causal relationship between variables. **a**, **c**, Based on data from years identified as collectively forcing grouse into synchronous increasing or peak states. **b**, **d**, Based on data from years identified as collectively forcing grouse into synchronous decreasing or trough states. The two parsimonious models are based on the red grouse climate hypothesis (**a**, **b**), and the red grouse climate–parasite hypothesis (**c**, **d**).

and climate–parasite (Fig. 3c and d) hypotheses—performed statistically well in both the 'upward' and 'downward' years, and there was no apparent statistical difference between them. For Fig. 3a, the generalized least squares (GLS) is 0.18, the probability that χ^2 of the observed hypothesis (H_{obs}) is bigger than the null hypothesis (H_{exp}), $P[\chi^2(H_{obs} > H_{exp})]$, is 0.83 and the corrected Akaike information criterion for small sample size (AIC_C) is 1.20. For Fig. 3c, GLS = 2.03, $P[\chi^2(H_{obs} > H_{exp})] = 0.86$ and $AIC_C = 1.55$. For Fig.3b, GLS = 4.76, $P[\chi^2(H_{obs} > H_{exp})] = 0.96$ and $AIC_C = 2.00$. For Fig. 3d, GLS = 7.33, $P[\chi^2(H_{obs} > H_{exp})] = 0.99$ and $AIC_C = 3.53$.

However, a closer examination of the estimated grouse–environment interaction coefficients showed that the climate model was not ecologically consistent with the data in Table 2. Indeed, this model proposed that for the set of 'upward' CFEs (Fig. 3a) grouse abundance increased owing to wetter Mays and drier Julys, and that for the set of 'downward' CFEs (Fig. 3b) grouse abundance decreased owing to warmer Mays and colder Julys. This contrasts with both the data summarized in Table 2 and previous field studies[15,25]. Thus the fit of the climate model is statistically reasonable but not biologically credible. The model based on the climate–parasite hypothesis was biologically consistent and in line with studies on the impact of weather both on grouse demography and on parasite transmission[11,15,19].

When applied to the set of 'upward' CFEs, the model revealed that relatively dry and warm Mays followed by cold and wet Julys were deleterious to parasite transmission, leading to low parasite intensities and positive red grouse growth rates. This collectively synchronized populations (Fig. 3c and Table 2). Within this model, climate also had a direct influence on grouse production, but the effect was less apparent. When applied to 'downward' CFEs, the climate–parasite model revealed that relatively wet Mays and warm Julys increased parasite transmission, which raised parasite intensity and led to a collective crash in grouse populations (Fig. 3d, Table 2). Dry and warm Mays impede the development of parasite eggs and the survival of the infective stage[19–21]. If these climatic conditions are followed by cold wet Julys, parasite development is further reduced[19–21]. Consequently, grouse feeding on the heather will have a low level of parasite infection, which results in an increase in grouse abundance and populations moving into a synchronous increase phase. In contrast, wet Mays and warm Julys favour abundant infective stages on the vegetation, leading to a rapid rise in the intensity of parasitic infection and causing a synchronous decline in grouse populations.

This study suggests that the effects of common climatic events on the density-dependent destabilizing interaction between host and parasite result in a phase synchrony between grouse populations. Our results also suggest that synchrony in grouse populations is an intermittent event, arising from populations that have been forced to converge into different phase states. These results have important implications for the management of natural populations and the control of infectious diseases because they indicate that certain weather conditions have a strong influence on eruptive outbreaks of infectious diseases or pest species and may lead to dramatic and synchronized changes in host abundance. □

Methods

Data sets

The red grouse time series provide one of the best data sets available on changes in relative abundance for examining spatio-temporal dynamics in animal populations. The time series are a good proxy for population abundance[13,28]. Furthermore, detailed population studies on red grouse have been undertaken and the fundamental mechanisms of population regulation identified and tested experimentally[6,11,25]. Each time series is based on a privately owned estate, the location of which was selected as the centre of the moorland habitat. For 60% of the time series we had corresponding time series of average intensity of *T. tenuis* infection in old and young red grouse randomly sampled between August and December for the period 1977–1994. *T. tenuis* intensity changes seasonally[19] but reaches an autumnal asymptote[29]. Monthly weather variables from April to August for the period 1839–1994, namely millimetres of rainfall and mean temperature in degrees Celsius, were provided as daily time series by the UK Met Office–British Atmospheric Data Centre service (http://badc.nerc.ac.uk/home). Rainfall records were from weather stations less then 10 km from each moor, while temperature came from stations less than 15 km away. Temperature time series were poorly represented, and so each series was reconstructed by scaling the series to the temperature expected at sea level (assuming temperature changes of 6.4 °C every 100 m). For each region and each month the new mean-temperature time series was calculated and then rescaled to the altitude of each original time series. (see Supplementary Information).

Spatio-temporal synchrony

Red grouse time series and climatic time series had occasional missing data points (1.3% of the total cases in red grouse) that were interpolated with a log-linear fit[14]. The red grouse data were normalized using a Box-Cox transformation and the long-term trend removed by selecting the residuals from fitting a non-parametric LOESS function to the data (the smoothing parameter included 75% of the observations and gaussian errors were assumed), thus leaving the short-term pattern unchanged. Parasite time series were $\log(x + 1)$-transformed and when fewer than three consecutive data points were missing they were replaced with the annual parasite mean from the local region. Significant collective forcing episodes were identified, and 95% confidence intervals were estimated from 5,000 bootstraps of the Shannon–Weaver index based on the state-based Markov chain model, using sample sizes of at least five time series per year[17]. We also carried out state-based Markov chain modelling for the parasite time series and the rainfall time series and found that the years of synchronous collective forcing in parasite time series coincided in 67% of the cases with synchronous CFEs for May rainfall and 50% of the cases with July rainfall (see Supplementary Information).

Causal mechanisms of synchrony

The structural equation model (SEM) was based on conceptual, inferential variables (known as latents) estimated through explanatory variables (known as manifests) represented by our time series. The SEM allowed us to explicitly account for environmental stochasticity and reciprocal relationships between variables, and as such correctly measures these latent variables and their interactions[26,27]. The explanatory variables inferring the weather variables were assumed to be fixed. Parameter identification and their 95% confidence intervals were estimated using bootstrap and Monte Carlo techniques (SEPATH, StatSoft) because the data violated some of the assumptions of structural equation modelling[26]. We first estimated the predicted model parameters and the χ-squared statistic for the generalized least-squares discrepancy function, using the correlation matrix of the original data set. We then carried out bootstrap extractions with replacement based on 50 samples and calculated the χ-squared statistic for the SEM simulated on these new data. Finally, we ran 1,000 Monte Carlo replications of these bootstrapped models and calculated the empirical probability $P(H_{obs} > H_{exp})$ and the 95% confidence intervals for the original model and its parameters (see Supplementary Information).

Received 13 July; accepted 15 December 2004; doi:10.1038/nature03276.

1. Cattadori, I. M., Merler, S. & Hudson, P. J. Searching for mechanisms of synchrony in spatially structured gamebird populations. *J. Anim. Ecol.* **69,** 620–638 (2000).
2. Grenfell, B. T. *et al.* Noise and determinism in synchronized sheep dynamics. *Nature* **394,** 674–677 (1998).
3. Post, E. & Forchammer, M. C. Synchronization of animal population dynamics by large-scale climate. *Nature* **420,** 168–171 (2002).
4. Ranta, E., Kaitala, V., Lindström, J. & Lindén, H. Synchrony in population dynamics. *Proc. R. Soc. Lond. B* **262,** 113–118 (1995).
5. Stenseth, N. C. *et al.* Common dynamic structure of Canada lynx populations within three climatic regions. *Science* **285,** 1071–1073 (1999).
6. Hudson, P. J., Dobson, A. P. & Newborn, D. Population cycles and parasitism. *Science* **286,** 2425a (1999).
7. Bjørnstad, O. N., Peltonen, M., Liebhold, A. M. & Baltensweiler, W. Waves of larch budmoth outbreaks in the European Alps. *Science* **298,** 1020–1023 (2002).
8. Ranta, E., Kaitala, V., Lindström, J. & Helle, A. The Moran effect and synchrony in population dynamics. *Oikos* **78,** 136–142 (1997).
9. Moran, P. A. P. The statistical analysis of the Canadian lynx cycle. II. Synchronization and meteorology. *Austr. J. Zool.* **1,** 291–298 (1953).
10. Greenman, J. V. & Benton, T. G. The impact of stochasticity on the behaviour of nonlinear population models: synchrony and the Moran effect. *Oikos* **93,** 343–351 (2001).
11. Hudson, P. J., Newborn, D. & Dobson, A. P. Regulation and stability of a free-living host–parasite system: *Trichostrongylus tenuis* in red grouse. I: Monitoring and parasite reduction experiments. *J. Anim. Ecol.* **61,** 477–486 (1992).
12. Dobson, A. P. & Hudson, P. J. Regulation and stability of a free-living host–parasite system: *Trichostrongylus tenuis* in red grouse. II: Population models. *J. Anim. Ecol.* **61,** 487–498 (1992).
13. Cattadori, I. M., Haydon, D. T., Thirgood, S. J. & Hudson, P. J. Are indirect measures of abundance a useful index of population density? The case of red grouse harvesting. *Oikos* **100,** 439–446 (2003).
14. Haydon, D. T., Shaw, D. J., Cattadori, I. M., Hudson, P. J. & Thirgood, S. J. Analysing noisy time series: describing regional variation in the cyclic dynamics of red grouse. *Proc. R. Soc. Lond. B* **269,** 1609–1617 (2002).
15. Hudson, P. J. *Grouse in Space and Time* (The Game Conservancy Trust, Fordingbridge, 1992).
16. Buonaccorsi, J. P., Elkinton, J. S., Evans, S. R. & Liebhold, A. M. Measuring and testing for spatial synchrony. *Ecology* **82,** 1668–1679 (2001).
17. Haydon, D. T., Greenwood, P. E., Stenseth, N. C. & Saitoh, T. Spatio-temporal dynamics of the grey-sided vole in Hokkaido: identifying coupling using state-based Markov-chain modelling. *Proc. R. Soc. Lond. B* **270,** 435–445 (2003).

18. Hudson, P. J. The effect of a parasitic nematode on the breeding production of red grouse. *J. Anim. Ecol.* **55,** 85–94 (1986).
19. Anderson, R. C. *Nematode Parasites of Vertebrates. Their Development and Transmission* 2nd edn (CABI, Wallingford, 2000).
20. Lee, D. L. *The Biology of Nematodes* (Taylor and Francis, London, 2002).
21. Marquardt, W. C., Demaree, R. S. & Grieve, R. B. *Parasitology and Vector Biology* (Harcourt Academic, San Diego, 2000).
22. Slagsvold, T. Production of young by the Willow Grouse *Lagopus lagopus* (L.) in Norway in relation to temperature. *Norw. J. Zool.* **23,** 269–275 (1975).
23. Mougeot, F., Redpath, S. M., Leckie, F. & Hudson, P. J. The effect of aggressiveness on the population dynamics of a territorial bird. *Nature* **421,** 737–739 (2003).
24. Watson, A., Moss, R. & Parr, R. Effect of food enrichment on numbers and spacing behaviour of red grouse. *J. Anim. Ecol.* **53,** 663–678 (1984).
25. Hudson, P. J. *et al.* Trophic interactions and population growth rates: describing patterns and identifying mechanisms. *Phil. Trans. R. Soc. Lond. B* **357,** 1259–1271 (2002).
26. Shipley, B. *Cause and Correlation in Biology* (Cambridge Univ. Press, Cambridge, 2000).
27. Pugesek, B. H., Tomer, A. & von Eye, A. *Structural Equation Modeling* (Cambridge Univ. Press, Cambridge, 2003).
28. Hudson, P. J., Dobson, A. P. & Newborn, D. in *Population Cycles* (ed. Berryman, A.) 109–129 (Oxford Univ. Press, Oxford, 2003).
29. Hudson, P. J. & Dobson, A. P. in *Infectious Diseases in Natural Populations* (eds Grenfell, B. T. & Dobson, A. P.) 144–176 (Cambridge Univ. Press, Cambridge, 1995).

Supplementary Information accompanies the paper on **www.nature.com/nature**.

Acknowledgements I.M.C. thanks D. Shaw for statistical advice. We are also grateful to D. Newborn of the Game Conservancy Trust, The Earl Peel and moor owners in northern England who allowed us to aggregate the database. O. Bjørnstad, E. Post and D. Johnson provided comments on an earlier version. I.M.C. was funded by a Marie Curie fellowship.

Competing interests statement The authors declare that they have no competing financial interests.

Correspondence and requests for materials should be addressed to I.M.C. (imc3@psu.edu).

Addition of human melanopsin renders mammalian cells photoresponsive

Z. Melyan[1], E. E. Tarttelin[1,2], J. Bellingham[2], R. J. Lucas[2] & M. W. Hankins[1]

[1]*Department of Visual Neuroscience, Division of Neuroscience and Psychological Medicine, Imperial College London, Charing Cross Hospital Campus, Fulham Palace Road, London W6 8RF, UK*
[2]*Faculty of Life Sciences, Michael Smith Building, University of Manchester, Manchester M13 9PT, UK*

A small number of mammalian retinal ganglion cells act as photoreceptors for regulating certain non-image forming photoresponses[1–10]. These intrinsically photosensitive retinal ganglion cells express the putative photopigment melanopsin[11–13]. Ablation of the melanopsin gene renders these cells insensitive to light[14]; however, the precise role of melanopsin in supporting cellular photosensitivity is unconfirmed. Here we show that heterologous expression of human melanopsin in a mouse paraneuronal cell line (Neuro-2a) is sufficient to render these cells photoreceptive. Under such conditions, melanopsin acts as a sensory photopigment, coupled to a native ion channel via a G-protein signalling cascade, to drive physiological light detection. The melanopsin photoresponse relies on the presence of *cis*-isoforms of retinaldehyde and is selectively sensitive to short-wavelength light. We also present evidence to show that melanopsin functions as a bistable pigment in this system, having an intrinsic photoisomerase regeneration function that is chromatically shifted to longer wavelengths.

In order to determine the function of melanopsin in an intact cellular environment, we examined the ability of heterologous expression of human melanopsin to render mammalian neuronal cells photoreceptive. Cells from the Neuro-2a mouse neuroblastoma cell line were transfected with plasmid expression vectors engineered to express both the complete coding sequence of human melanopsin under control of the immediate early promoter of cytomegalovirus (CMV), and an enhanced green fluorescent protein (EGFP) reporter gene driven by an SV40 enhancer/promoter. High transfection efficiencies were obtained using the lipofectamine technique, with up to 60% of Neuro-2a cells expressing EGFP as assessed by fluorescence microscopy. Untransfected Neuro-2a cells did not express melanopsin (or rod/cone opsins) in either their differentiated or undifferentiated states (see Supplementary Fig. 1). After plasmid transfection, human melanopsin was observed at both the mRNA and protein level (Fig. 1b; see Supplementary Figs 1 and 2).

Because opsin photopigments use *cis*-isoforms of retinaldehyde as a chromophore, physiological light responses were first assessed following pre-incubation with commercially available 9-*cis*-retinaldehyde (1 h, 20 μM). A 10 s stimulus of 420-nm light (20-nm half-bandwidth) resulted in a sustained inward current (recovering over >10 min), which was not observed in untransfected cells or cells transfected with a control vector lacking melanopsin (Fig. 1d, e). The magnitude of the response was irradiance-dependent (Fig. 1d), and under voltage ramps had a peak slope conductance for the brightest stimulus of 6.46 ± 0.82 nS (mean ± s.e.m., $n = 13$), some three times greater than previously observed in intrinsically photosensitive retinal ganglion cells (ipRGCs) following exposure to a stimulus of similar intensity[5].

The photoreceptive function of melanopsin was dependent on the presence of an appropriate isoform of retinaldehyde (Fig. 2a). In the absence of exogenous retinaldehyde, melanopsin-transfected cells were not light-sensitive. Significant photosensitivity was observed following pre-incubation with either 9-*cis*- or 11-*cis*- but not with all-*trans*-retinaldehyde.

These findings are consistent with the hypothesis that melanopsin acts as a photopigment with a specific affinity for *cis*-isoforms of retinaldehyde. However, application of all-*trans*-retinaldehyde in this preparation also seemed to support a modest light response (Fig. 2a). Phylogenetically, melanopsin is most closely related to the cephalopod rhodopsins[15], which use 11-*cis*-retinaldehyde as a chromophore for sensory functions but are also capable of binding all-*trans*-retinaldehyde, which they re-isomerize to 11-*cis*-retinaldehyde upon appropriate light exposure[16]. Such an isomerase function would facilitate photosensitivity following incubation with all-*trans*-retinaldehyde provided that the test stimulus was of sufficient duration to generate a *cis*-isoform in the first instance.

To examine the possibility that melanopsin has a similar inherent chromophore regeneration capability, we assessed the ability of prior light exposure with a wavelength outside the response range of 9- or 11-*cis*-retinaldehyde-loaded cells (Fig. 3a) to facilitate photosensitivity of cells loaded with all-*trans*-retinaldehyde. Exposure to 540-nm light had no effect on membrane current, but responses of cells loaded with all-*trans*-retinaldehyde to a test stimulus of 420-nm light were greatly enhanced following exposure to the longer wavelength light (Fig. 2b–d). The hypothesis that this sensitization is caused by a photoisomerization of the all-*trans*-retinaldehyde to a *cis*-isomer is supported by the observation that 540-nm light had no effect on the responses of cells loaded with 11-*cis*-retinaldehyde. Interestingly, a small increase in photosensitivity was observed in 9-*cis*-retinaldehyde-loaded cells treated with 540-nm light. This would be predicted if photoisomerization resulted in the generation of 11-*cis*-retinaldehyde, as opsin photopigments incorporating this isoform are commonly more sensitive[17] (Fig. 2a).

Neuro-2a cells do not express either of the known mammalian photoisomerases (RGR-opsin[18] and peropsin), as determined by